IEEE Access
Multidisciplinary | Rapid Review | Open Access Journal

Received 27 October 2023, accepted 11 November 2023, date of publication 14 November 2023,
date of current version 21 November 2023.

Digital Object Identifier 10.1109/ACCESS.2023.3332731

RESEARCH ARTICLE

Machine Learning Techniques for Predicting Metamaterial Microwave Absorption Performance: A Comparison

PRINCE JAIN[1], HIMANSHU CHHABRA[1], URVASHI CHAUHAN[2], KRISHNA PRAKASH[3], PIYUSH SAMANT[4], DHIRAJ KUMAR SINGH[5], MOHAMED S. SOLIMAN[6], (Senior Member, IEEE), AND MOHAMMAD TARIQUL ISLAM[7], (Senior Member, IEEE)

[1]Department of Mechatronics Engineering, Parul Institute of Technology, Parul University, Vadodara, Gujarat 391760, India
[2]Department of Electronics and Communication Engineering, Parul University, Vadodara, Gujarat 391760, India
[3]Department of Electronics and Communication, NRI Institute of Technology, Vijayawada, Andhra Pradesh 521212, India
[4]Research and Development, Mirxes Laboratories Pvt. Ltd., Singapore 138667
[5]Kalpana Chawla Centre for Research in Space Science and Technology, Chandigarh University, Mohali, Punjab 140413, India
[6]Department of Electrical Engineering, College of Engineering, Taif University, Taif 21944, Saudi Arabia
[7]Department of Electrical, Electronic and Systems Engineering, Faculty of Engineering and Built Environment, Universiti Kebangsaan Malaysia, Bangi, Selangor 43600, Malaysia

Corresponding authors: Prince Jain (princeece48@gmail.com) and Mohammad Tariqul Islam (tariqul@ukm.edu.my)

This work was supported in part by the Ministry of Higher Education (MOHE), Malaysia, through the Fundamental Research Grant Scheme (FRGS), under Grant FRGS/1/2021/TK0/UKM/01/6; and in part by the Deanship of Scientific Research, Taif University, Saudi Arabia.

ABSTRACT This work presents a metamaterial absorber (MMA) for X- and Ku-bands with a metallic resonating patch on top and a ground plane separated by substrate FR-4 with a thickness of 0.053 λ at the lowest resonance frequency. The proposed MMA demonstrates perfect absorption of 99.42, 98.48, 98.92, and 99.34 % at 9.948, 13.26, 14.92, and 15.80 GHz, respectively at normal incidence. The proposed MMA demonstrates perfect absorption for a polarization and incident angle over a wide range of angles up to 45°. To understand the fundamental EM behavior of the metamaterial structure, equivalent circuit analysis was carried out, and the circuit outputs accorded with the simulation results. This article also compares various machine learning (ML) methods for optimizing the design and predictive modeling of MMAs, such as decision trees, K-nearest neighbors, random forests, extra trees (ET), bagging, LightGBM, XGBoost, hist gradient boosting, cat boost, and gradient boosting regressors. The primary objective is to assess the usefulness of each regressor technique in estimating the performance of MMAs using multiple tests ranging from TC-40 to TC-80 and performance metrics such as adjusted R-squared score, MSE, RMSE, and MAE, in which the ET regressor excels. Simulation results suggest that ML-based techniques can save simulation resources and time while still being an efficient tool for predicting absorber behavior at intermediate and subsequent frequencies.

INDEX TERMS Decision tree, equivalent circuit analysis, extra trees, machine learning, metamaterial absorber, random forest.

I. INTRODUCTION

Due to the unbelievable properties of metamaterial which are not found in nature, metamaterials have been widely used in various applications like invisibility cloaks [1], electromagnetic wave absorbers [2], sensing [3], modulators [4], antennas, and so on. Metamaterial has emerged as an ideal alternative for fulfilling the demands of advanced absorber applications owing to its remarkably thin profile, compact nature, and ability to achieve complete absorption. These exceptional characteristics make MMA promising for wide applications, such as energy harvesting [5], sensing [6], [7],

The associate editor coordinating the review of this manuscript and approving it for publication was Qi Luo.

satellite communication [8], photodetector [9], microwave imaging [10], stealth technology [11], IoT applications and many more.

Metamaterial absorbers have been around since 2002, when Engheta first came up with the idea of using metamaterial surfaces on screens to absorb electromagnetic waves [12]. In 2008, Landy developed a highly efficient metamaterial absorber (MMA) [2]. Subsequently, metamaterial absorbers (MMAs) have garnered significant interest due to their exceptional capacity for electromagnetic (EM) wave absorption [13], [14]. MMAs are often structured in periodic configurations consisting of resonators that are fabricated on a substrate, while a ground plane is located at the lowermost position. The metallic resonator and dielectric substrate are excited by the incident electric and magnetic field, respectively [2]. These structures can minimize the reflection by matching the impedance of the MMA to free space and the transmission is eliminated by the ground plane to achieve perfect absorption [3].

Till now, various metamaterial-based structures have been investigated, including split-ring structures [15], ring-shaped [16], square-shaped [17], cut-wire [18], Gemini-shaped [13] and spilt-Jerusalem cross resonator [19] to demonstrate their performance with dual- [15], [16], multi- [13], [17], [19], and broad-band [20] operations. To achieve a multi-band absorption performance, several efforts have been carried out using orthogonal arrangements of different metallic resonators [18], [20] or multi-layer metallic structures separated by dielectric substrates [17], [21]. Recently, a single-layer triple-band absorber is proposed utilizing three concentric closed circular ring resonators in a unit cell [15]. Nevertheless, these techniques can face technical challenges during the manufacturing process, thereby substantially impacting their feasibility for real-world applications. In addition, several MMAs with polarization-sensitive characteristics have been demonstrated and drawn significant attention due to their applications in polarization detection and imaging [18], [19].

The majority of MMA modeling analysis depends on EM simulation software like High-frequency Structure Simulator (HFSS) and Computer Simulation Technology (CST), which are based on iterative numerical full wave calculations such as the Finite Element Method (FEM) [22], and Finite-Difference Time-Domain (FDTD) [23]. Designing metamaterial absorbers with optimal performance remains a significant challenge due to the involvement of large trial and error searches over geometric dimensions, which necessitates the validation and optimization of each parameter. Extensive modeling techniques are needed to precisely estimate the absorber's performance because of the complex relationship between the structural elements of the absorber and its absorption characteristics. A recent study has demonstrated a significant increase in the application of machine learning regressor techniques to enhance the predictive modeling of metamaterial absorber performance, enabling an improved understanding of patterns and behaviors in photonics devices [6]. Regression analysis is a statistical methodology employed to determine the connection between a dependent variable, namely absorption value, and an independent variable, specifically frequency. Because of their ability to capture complex relationships among data, decision tree (DT), random forest (RF), K-nearest neighbors (KNN), extra trees (ET), bagging, light gradient boosting machine (LGBM), extreme gradient boosting (XGB), hist gradient boosting (HGB), cat boost (CBR) and gradient boosting (GBR) regressors techniques have emerged as attractive methods. The regressor methods have demonstrated their efficacy in various applications, such as electromagnetic wave analysis and material characterization. The absorption and reflection response of photonic devices can also be observed and predicted using machine learning [6]. Several studies have explored the use of machine learning in various applications related to antenna designs, metamaterials for target adaptation, and manufacturing process optimization [24], [25]. ML techniques offer faster simulations while achieving the same levels of precision [26]. Since then, MMA structures have been demonstrated with different applicable ML regression algorithms, such as Extra trees [6], XGBoost [27], and k-nearest neighbor regressor [28].

This study presents a compact and ultra-thin metamaterial absorber that exhibits ideal absorption characteristics in X- and Ku-band applications. The MMA exhibits quad absorption peaks *i.e.* one (9.948 GHz) in X-band and three (13.26, 14.92, and 15.80 GHz) in Ku-band. The primary objective of this study is to address the existing research gap through a comprehensive evaluation and comparison of different well-known regression techniques for metamaterial absorbers, which represents a novel contribution. The aim is to identify the most efficient approach for optimizing the design and predictive modeling of metamaterial absorbers for microwave applications. The absorption dataset is initially split into separate training and testing sets, followed by the utilization of regression models to effectively forecast absorption. The study conducts a comparative evaluation of multiple regression models, specifically DT, KNN, RF, ET, bagging, XGB, LGBM, HGB, CBR, and GBR models. Various performance metrics, including root mean squared error (RMSE), mean absolute error (MAE), mean squared error (MSE), and Adjusted R-squared, are employed to determine the optimal regressor technique for precise prediction modeling of metamaterial absorber performance in microwave applications. The findings of the comparative analysis indicate that the Extra Trees Regressor demonstrates superior predictive capabilities compared to other models across all test sizes.

II. DESIGN AND RESULTS DISCUSSIONS

The proposed MMA configuration comprises a circular enclosure containing T-shaped resonator that have been altered to achieve complete absorption at four distinct resonant frequencies. As shown in Figure 1(a), the unit cell is made up of a metallic resonator and a copper ground plane that is isolated by a FR4 substrate. The loss tangent and permittivity values for the FR4 substrate are reported as 0.02 and

4.4, respectively. Furthermore, copper has a conductivity (σ) value of 5.8×10^7 S/m. The metallic layer has a thickness of 0.035 mm (h_c), while the dielectric layer has a thickness of 1.6 mm (h_s). The top view of the MMA with optimized parameters are a = 12.2 mm, b = 7.6 mm, c = 2.88 mm, g = 0.8 mm, r_i =4.8 mm, and r_o = 5.6 mm as shown in Fig. 1(b). At the lowest resonance frequency, the absorber is compact (0.406 λ) and thin (0.053 λ). The occurrence of electric and magnetic fields excites the MMA, resulting in variations to its effective permittivity (ε_{eff}) and effective permeability (μ_{eff}). The absorption phenomenon at different resonant frequencies is observed when the incident wave's electric and magnetic fields act simultaneously, as depicted in Figure 1(c).

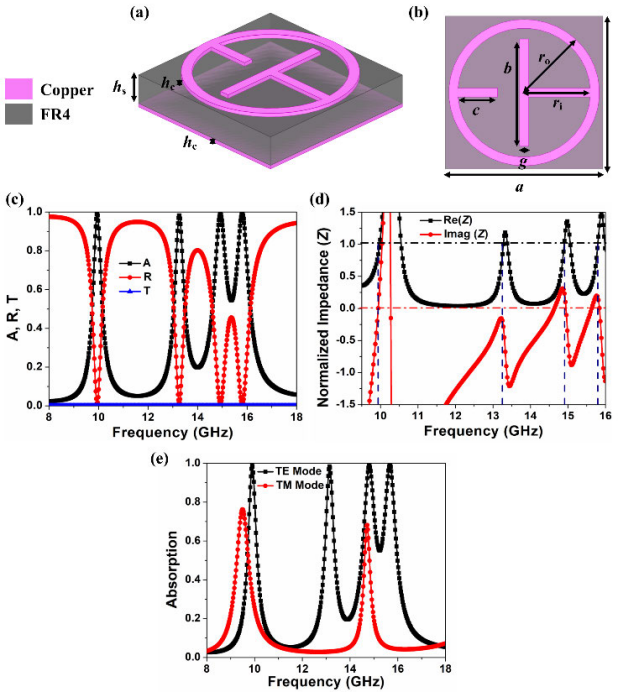

FIGURE 1. (a) Perspective view, (b) Top View, (c) Absorption (A), reflection (R) and transmission (T) response, and (d) Real and imaginary normalized impedance (e) Absorption response for TM and TE mode of the proposed metamaterial absorber.

The absorption coefficient can be determined using $A = \sqrt{1 - |S_{11}|^2 - |S_{21}|^2}$, where S_{11} and S_{21} are the reflection coefficient and transmission coefficient, respectively. Nevertheless, the presence of a metallic ground plane results in zero transmission, leading to the equation $A = \sqrt{1 - |S_{11}|^2}$. The expression for the reflection coefficient is given by $\left|(Z - Z_0)/(Z + Z_0)\right|^2$, where Z_0 and Z are the free space and MMA impedance. The absorption will be perfect by optimizing the geometrical structure and its dimensions [15]. The reflection (R), absorption (A), and transmission (T) characteristics are depicted in Figure 1(c), showcasing peak absorptivity values of 99.42%, 98.48%, 98.92%, and 99.34% at resonating frequencies of 9.94 (f_1), 13.26 (f_2), 14.92 and 15.80 GHz (f_3), respectively. In order to reduce the chance of reflection, it is desirable for the real and imaginary components of the normalised impedance to converge towards values of one and zero, respectively. The normalized impedance (Z) is 0.85+j0.01, 0.92-j0.22, 1.15+j0.16 and 1.01+j0.17 at 9.948, 13.26, 14.92, and 15.80 GHz, respectively, as shown in Fig. 1(d). The absorption performance of the MMA under TM and TE polarization is depicted in Fig. 1 (e), where the absorptivity at resonant frequencies of 9.47 and 14.74 GHz is 76.1 and 68.4%, respectively, for TM polarization, demonstrating the polarisation dependence of the proposed MMA.

Commercially available software like as ADS can be utilized to create the equivalent circuit of the MMA, as shown in Fig. 2. Due to the presence of capacitive gaps between the resonators, L and C values must be integrated as parallel transmission lines connected by a capacitive element between them for each resonance frequency. Four parallel R-L-C circuits were needed to accommodate the four resonance frequencies. To match the corresponding absorption values obtained from the HFSS simulation, the R values for each R-L-C circuit (for each resonance frequency) were adjusted using the ADS circuit simulator. Since MMAs exhibit periodicity, they may enable electromagnetic coupling through the presence of inductive and capacitive components within the circuit. Introducing series capacitances (C_5, C_6, C_7, and C_8) in the circuit, as presented in Fig. 2 (a), can eliminate this issue. The values of capacitors C_5, C_6, C_7, and C_8 were adjusted through fine-tuning using the ADS circuit simulator to attain optimal isolation within the bands located between resonance frequencies. The resonance frequencies in the output obtained from the equivalent circuit and HFSS simulation exhibit a high level of resemblance suggesting a strong agreement in terms of absorption, as illustrated in Fig. 2 (b).

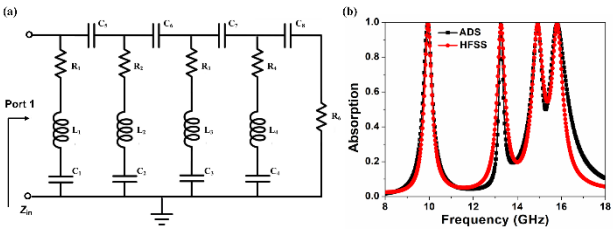

FIGURE 2. (a) Equivalent circuit Model (ECM) of the proposed MMA, R_1 = 41.29 Ω, R_2 = 27.06 Ω, R_3 = 16.67 Ω, R_4 = 27.08 Ω, R_5 = 50 Ω, R_6 = 50 Ω, L_1 = 28.60 nH, L_2 = 36.70 nH, L_3 = 6.30 nH, L_4 = 39.6 nH, C_1 = 0.009 pF, C_2 = 0.004 pF, C_3 = 0.0291 pF, C_4 = 0.002 pF, C_5 = 0.167 pF, C_6 = 0.039 pF, C_7 = 0.015 pF, and C_8 = 0.027 pF, (b) Absorption response from ADS and HFSS.

The proposed MMA has been validated for various polarization (ϕ) and incident (θ) angles for TE polarization as depicted in Figure 3. The X- and Ku-band exhibit peaks at frequencies of 9.94, 13.26, 14.92, and 15.80 GHz under the condition of $\phi = 0^{\text{o}}$. The amplitude of the peaks decreases gradually with an increase in the polarization angle, which can be attributed to the asymmetrical characteristics of the structure, as depicted in Figure 3(a). The polarization-sensitive nature of the structure demonstrates the

TABLE 1. Comparative performance with Multi-Band MMAs reported in prior studies.

Ref.	Resonances	Lowest frequency (GHz)	Absorption (%) at f_{lowest}	Unit Cell size (mm)	Dielectric Thickness (mm)
S. R. Thummaluru et al.[29]	Dual	4.2	91	0.392 λ	0.0224 λ
D. Singh et al.[16]	Dual	17	~ 100	0.487 λ	0.022 λ
G. Deng et al.[30]	Triple	101.25	92.5	0.493 λ	0.016 λ
K.P. Kaur et al.[31]	Triple	1.8	98.96	0.209 λ	0.029 λ
K.P. Kaur et al.[21]	Triple	1.75	96.91	0.2 λ	0.037 λ
F. S. Jafari et al.[32]	Triple	8.6	~ 100	0.688 λ	0.045 λ
Proposed work	Quad	9.94	99.42	0.406 λ	0.053 λ

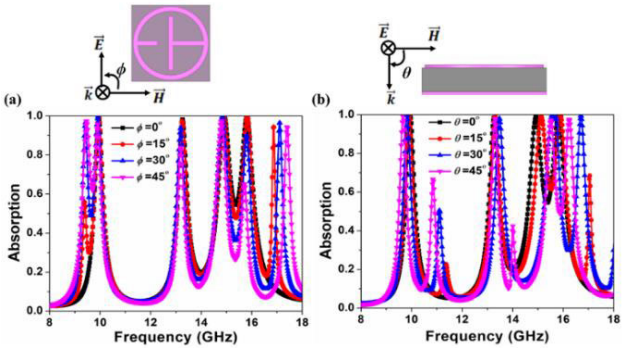

FIGURE 3. Absorption characteristics for different (a) polarization (ϕ), and (b) incident angles (θ).

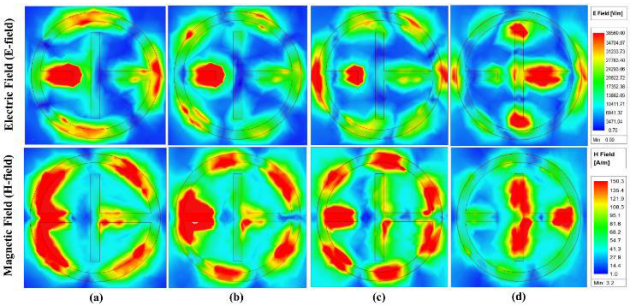

FIGURE 4. Electric field, and magnetic field distribution of the MMA at (a) 9.94, (b) 13.26, (c) 14.92, and (d) 15.80 GHz.

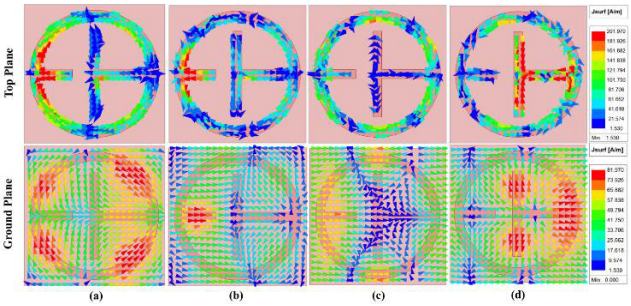

FIGURE 5. Surface current distribution for the top plane and ground plane of the MMA at (a) 9.94, (b) 13.26, (c) 14.92, and (d) 15.80 GHz.

practical applications in various fields including polarization detection and sensing [14], [19]. Moreover, it can be observed that the absorber exhibits insensitivity to incident angles up to 30 degrees. However, beyond this threshold, the rate of absorption diminishes as the angle increases, as depicted in Figure 3(b). Moreover, an analysis has been conducted on the electric field (E-field), magnetic field (H-field), and distribution of surface current to gain a comprehensive understanding of the absorption peaks. Figs. 4 (a) and (b) show that the simultaneous excitation of E-field and H-field distribution on the top plane resonator creates absorption peaks at 9.94, 13.26, 14.92, and 15.80 GHz. Figs. 5 (a) and (b) demonstrates the surface current on top and ground plane are anti-parallel and responsible for the magnetic coupling [33]. Nevertheless, the simultaneous excitation of both E- and H-fields leads to a significant enhancement in absorption performance. Table 1 presents a comparison of the proposed metamaterial absorber (MMA) with respect to the dimensions of the unit cell, specifically the size and thickness. The results indicate that the proposed MMA exhibits a compact and ultra-thin structure, which distinguishes it from previously reported multi-band absorbers.

III. MACHINE LEARNING REGRESSION MODELS

Regression models are powerful tools that can significantly reduce the time and resources needed to simulate complex systems. By using machine learning techniques, regression models can predict critical parameters and identify missing values. The process involves simulating the design, creating a comprehensive dataset, training the regression model, and predicting values for intermediate frequencies. Python is commonly used for implementing these regression models using simulated data.

A. SIMPLE REGRESSION MODELS

The relationships between the input parameters and the desired characteristics of the metamaterial absorbers can be understood with the help of simple regression models. In particular, we employ Decision trees and k-nearest neighbors regression techniques to capture and quantify the linear and nonlinear dependencies within the data. Decision trees are a simple and user-friendly method for ML that may be applied to both regression and classification applications. The process involves the recursive partitioning of data into increasingly smaller subsets, to achieve homogeneity within each subset. This can be a decent choice for regression situations with inadequate information, but it is prone to overfitting if not

carefully tuned [34], [35]. The k-nearest neighbors (KNN) algorithm is a non-parametric approach in machine learning that can be effectively employed for both classification and regression tasks. The functioning of this method involves identifying the k instances in the training dataset that exhibit the highest similarity to a novel instance. Subsequently, the label of the novel instance is predicted by considering the descriptions of the KNN. This can be an adequate option for regression problems with insufficient information, but it can be computationally expensive for large datasets [36].

B. BAGGING-BASED ENSEMBLE MODELS

Ensemble learning techniques are used to improve the robustness and generalisation of our metamaterial absorber optimisation models. Bagging-based Ensemble Models, such as Random Forest, Extra Trees and Bagging, are especially good at reducing overfitting and improving predictive accuracy. Random forest is an ML ensemble approach that mixes numerous decision trees to increase prediction accuracy. They operate by training several decision trees on distinct random selections of the training data and then averaging the individual tree's predictions. This can be a suitable solution for regression problems with inadequate data because it is less prone to overfitting than single decision trees [37], [38]. Extra trees are a random forest variant that employs a more randomized technique to train individual trees [39]. This has the potential to improve forecast accuracy, particularly in high-dimensional datasets [6], [40]. Bagging regression technique combines many copies of a basic model, each trained on a separate bootstrap sample of the training data. This can help to improve forecast accuracy by reducing the variance of the fundamental model. However, Bagging might be computationally expensive for huge datasets [41].

C. BOOSTING-BASED ENSEMBLE MODELS

Boosting-based Ensemble Models iteratively combine weak learners to create a strong predictive model to improve model performance. The light gradient boosting machine (LightGBM) Regressor is well-known for its speed and effectiveness, particularly in instances with sparse datasets [42]. The XGBoost Regressor (Extreme Gradient Boosting) is an iterative procedure that integrates extra trees into the model to correct faults produced by previous trees. XGBoost is well-known for its remarkable computing efficiency and great predicted accuracy, particularly when dealing with large datasets [27]. The CatBoost algorithm targets categorical features to use the gradient boosting algorithm and integrates several methodologies to improve the algorithm performance when applied to datasets with categorical variables [43]. Histogram-based gradient boosting makes use of histograms to represent the features of a given dataset. When applied to datasets with categorical features, this approach has the potential to improve the algorithm's performance [44]. Gradient boosting regressors are specifically developed for regression problems, and they work by iteratively adding new trees into the model to correct errors produced by previous trees [45].

These regression algorithms can be assessed using several performance metrics, including MSE, RMSE, MAE, and Adjusted R-squared score (Adj-R^2S). These metrics reveal the model's tendency for generalization, goodness-of-fit, and forecasting accuracy for MMAs. The subsequent equations can be employed to ascertain these performance indices:

$$R^2S = 1 - \frac{\sum_{i=1}^{N} (Predicted\ Value_i - Actual\ Value_i)^2}{\sum_{i=1}^{N} (Actual\ Value_i - Average\ Target\ Value_i)^2} \tag{1}$$

$$Adj - R^2S = 1 - \frac{(1 - R^2S)(N-1)}{N-p-1} \tag{2}$$

$$MSE = \frac{1}{N} \sum_{i=1}^{N} (Actual\ Value_i - Predicted\ Value_i)^2 \tag{3}$$

$$RMSE = \sqrt{\frac{1}{N} \sum_{i=1}^{N} (Actual\ Value_i - Predicted\ Value_i)^2} \tag{4}$$

$$MAE = \frac{1}{n} \sum_{i=1}^{n} \left| \frac{Actual\ Value_i - Predicted\ Value_i}{Actual\ Value_i} \right| \tag{5}$$

where 'N' is the total number of samples used in the regression model's validation.

Regression models were used to forecast the absorption coefficient value for various test sizes. The regression model was trained with 60% of the records and its prediction performance was tested with 40% of the records for the 40% test size. Similarly, with the 80% test size, the regression model was trained on a sample of 20% of the records before being tested on the remaining 80%. This technique was repeated with test sizes ranging from 50% to 70%.

IV. RESULTS AND DISCUSSIONS

The Adjusted-R^2 scores for various regression algorithms utilizing test sizes ranging from 40% to 80% of the data set are shown in Figure 6. The Adjusted-R^2 score is commonly used for assessing the goodness of fit of regression models, taking into account both the model's ability to explain variance in the data and the number of predictors utilized. Adjusted-R^2 values near 1 imply a stronger link between predicted and actual values. As the test size increased from 40% to 80% of the dataset, the adjusted-R^2 scores for all regression methods decreased suggesting that the percentage of training and testing data affects the model's prediction performance. Across all test sizes, the extra trees regressor consistently achieved the best adjusted-R^2 scores, indicating higher predictive performance. This regressor combines the advantages of randomization and extreme random splitting, resulting in decision trees with a higher amount of randomness and diversity. The enhanced randomization enables the

additional trees regressor to capture a greater range of patterns while reducing overfitting. The RF regressor also performed well as it constructs a decision tree ensemble with random subsets of features and data samples, decreasing overfitting and improving generalization.

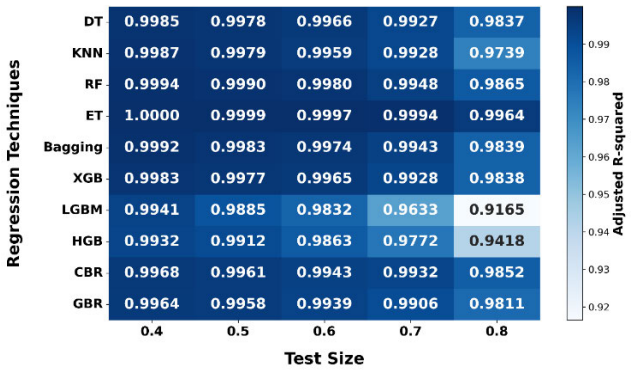

FIGURE 6. Adjusted-R^2 for decision tree (DT), K-nearest neighbors (KNN), random forest (RF), extra trees (ET), bagging, XGBoost, LightGBM, hist gradient boosting (HGB), cat boost (CBR) and gradient boosting (GBR) regressors with test sizes ranging from 40% to 80% of the dataset.

TABLE 2. Mean absolute error (MAE) values.

Regression Techniques	Test Sizes				
	0.4	0.5	0.6	0.7	0.8
DT	0.0065	0.0078	0.0089	0.0118	0.0182
KNN	0.0050	0.0067	0.0091	0.0127	0.0228
RF	0.0038	0.0047	0.0061	0.0092	0.0151
ET	0.0007	0.0011	0.0016	0.0025	0.0062
Bagging	0.0042	0.0055	0.0069	0.0103	0.0163
XGB	0.0071	0.0084	0.0092	0.0120	0.0184
LGBM	0.0117	0.0161	0.0215	0.0344	0.0565
HGB	0.0119	0.0145	0.0183	0.0264	0.0473
CBR	0.0085	0.0090	0.0105	0.0123	0.0177
GBR	0.0110	0.0119	0.0132	0.0155	0.0210

TABLE 3. Mean squared error (MSE) values.

Regression Techniques	Test Sizes				
	0.4	0.5	0.6	0.7	0.8
DT	0.0001	0.0002	0.0003	0.0006	0.0014
KNN	0.0001	0.0002	0.0003	0.0006	0.0022
RF	0.0000	0.0001	0.0002	0.0004	0.0011
ET	0.0000	0.0000	0.0000	0.0000	0.0003
Bagging	0.0001	0.0001	0.0002	0.0006	0.0011
XGB	0.0001	0.0002	0.0003	0.0006	0.0014
LGBM	0.0005	0.0009	0.0014	0.0030	0.0071
HGB	0.0006	0.0007	0.0011	0.0019	0.0049
CBR	0.0003	0.0003	0.0005	0.0006	0.0012
GBR	0.0003	0.0003	0.0005	0.0008	0.0016

The MAE, MSE, and RMSE performance metrics for various regression techniques are shown in Table 2, 3 and 4. The accuracy of regression models is assessed using these metrics, which involve the examination of discrepancies between

TABLE 4. Root mean squared error (RMSE) values.

Regression Techniques	Test Sizes				
	0.4	0.5	0.6	0.7	0.8
DT	0.0109	0.0135	0.0167	0.0245	0.0372
KNN	0.0102	0.0131	0.0183	0.0244	0.0470
RF	0.0067	0.0095	0.0130	0.0209	0.0343
ET	0.0013	0.0020	0.0038	0.0053	0.0147
Bagging	0.0081	0.0109	0.0132	0.0222	0.0390
XGB	0.0116	0.0138	0.0168	0.0243	0.0370
LGBM	0.0218	0.0307	0.0370	0.0551	0.0841
HGB	0.0235	0.0268	0.0334	0.0434	0.0702
CBR	0.0161	0.0180	0.0216	0.0238	0.0353
GBR	0.0170	0.0185	0.0222	0.0279	0.0400

predicted and actual values. Lower values are indicative of superior predictive performance. Between 40% and 80% of the dataset was tested in various test sizes during the evaluation. Table 2 shows ET and RF regressors consistently produced relatively low MAE values across all test sizes, with ET achieving MAE as low as 0.0007 and RF as low as 0.0038 for a test size of 0.4. In contrast, LGBM and HGB regressors exhibited higher MAE values, especially as the test size increased, suggesting that they may be more sensitive to larger test datasets. Table 3 and 4 shows that ET and RF regressors produced consistently low MSE and RMSE values across all test sizes. On the other hand, LGBM and HGB regressors had higher MSE and RMSE values, especially as the test size increased. Across all test sizes, the extra trees regressor consistently recorded the lowest MSE, RMSE, and MAE scores, demonstrating its superior predictive ability. This can be attributed to the extra trees regressor's ability to leverage randomization and extreme random splitting, adding more randomness and variety to the decision trees. Similarly, the KNN and RF regressor also demonstrated competitive results with relatively low error values. These observations emphasize the effectiveness of different regression techniques and the need for careful selection based on the specific dataset characteristics and desired predictive accuracy.

Figure 7 presents scatter plots illustrating the relationship between predicted and simulated absorption values for different regression models including DT, KNN, RF, ET, bagging, XGB, LGBM, HGB, CBR, and GBR regressors with test sizes of 0.4, 0.5, and 0.6. Among these ensemble models, the Extra Tree regressor consistently exhibits the best results in accurately predicting the absorption values. These figures show how well ensemble models and other regression models perform in predicting absorption values across a range of test sizes. The scatter plots provide visual representations of the model's performance, accuracy, and overall trends. The inclusion of multiple test sizes from 0.4 to 0.6, enables an in-depth investigation of the model's performance when training and testing data are in varying proportions.

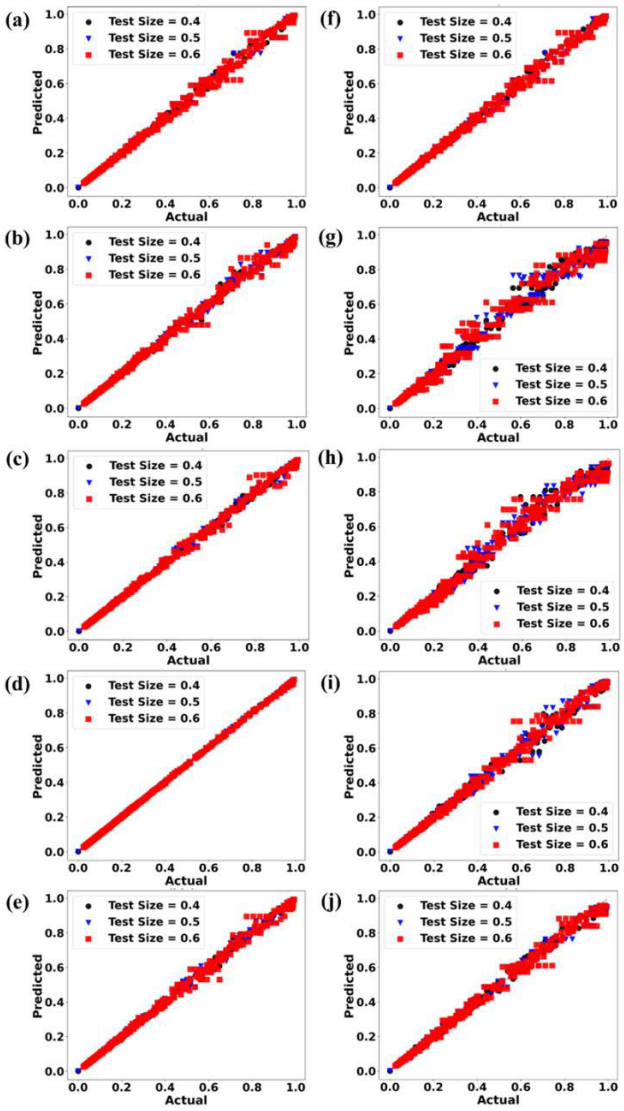

FIGURE 7. Scatter plots illustrating the relationship between predicted and simulated absorption values of (a) DT, (b) KNN, (c) RF, (d) ET, (e) bagging, (f) XGB, (g) LGBM, (h) HGB, (i) CBR and (j) GBR regressors for different test sizes 0.4, 0.5, and 0.6.

In Figure 8, we present a comparative analysis of computational times for various machine learning regression techniques when applied to a test dataset with a size of 40%. Notably, DT and KNN demonstrate remarkable computational efficiency, with execution times of 0.00485 seconds and 0.00459 seconds, respectively. Extra Trees also exhibited competitive computational performance, with an average time of 0.16044 seconds. These findings suggest that DT, KNN, and ET are well-suited for scenarios where rapid predictions are crucial. The longer computational times of CBR and LGBM, at 0.6938 seconds and 0.6061 seconds, respectively, show that despite their superior predictive performance, these models demand more computational power. These computational trade-offs should be taken into account by researchers when choosing regression techniques for particular applications.

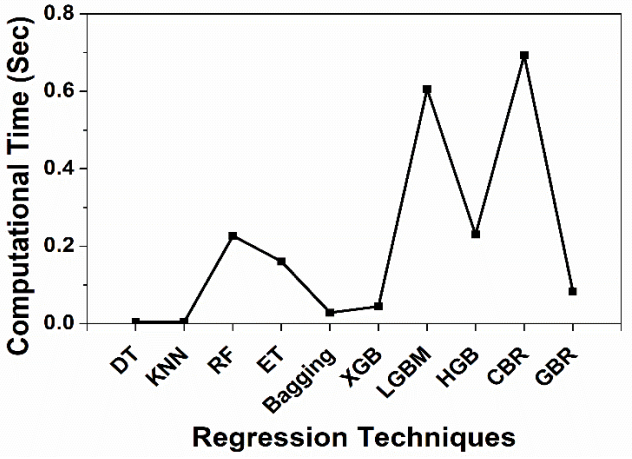

FIGURE 8. Computational time comparison of various machine learning regression techniques for test size of 40%.

V. CONCLUSION

The ultra-thin MMA at microwave frequencies exhibited four distinct peaks of perfect absorption, occurring at frequencies of 9.948, 13.26, 14.92, and 15.80 GHz. The absorption mechanism can be understood by examining the normalized impedance, E-field, H-field, and surface current distribution. In contrast to absorbers that have been previously reported, the proposed compact and ultrathin absorber exhibits perfect absorption at all resonant frequencies. The analysis of the equivalent circuit was carried out to explain the fundamental electromagnetic behavior of the proposed absorber. This study shows the rapid growth of MMAs but traditional design methods are time- and computationally intensive, making optimization difficult. To address this, this article provides a comprehensive comparative analysis of various ML regressors such as DT, KNN, RF, ET, bagging, XGB, LGBM, HGB, CBR, and GBR regressors in forecasting the performance of metamaterial absorbers. The ET regressor demonstrates outstanding performance in predicting MMA performance for an 80% test size with RMSE of 0.0147, MAE of 0.0062, MSE of 0.003, and an Adjusted R^2 of 0.9964. Overall, this study has significant implications for optimizing metamaterial absorber designs for microwave applications such as polarization imaging, detection, sensing, and stealth technology using ML regressor approaches.

ACKNOWLEDGMENT

The authors acknowledge the Fundamental Research Grant Scheme (FRGS), grant number FRGS/1/2021/TK0/UKM/01/6 funded by the Ministry of Higher Education (MOHE), Malaysia. The researchers would also like to acknowledge Deanship of Scientific Research, Taif University, Saudi Arabia for funding this work.

REFERENCES

[1] S. S. Islam, M. R. I. Faruque, and M. T. Islam, "An object-independent ENZ metamaterial-based wideband electromagnetic cloak," *Sci. Rep.*, vol. 6, no. 1, p. 33624, Sep. 2016, doi: 10.1038/srep33624.

[2] N. I. Landy, S. Sajuyigbe, J. J. Mock, D. R. Smith, and W. J. Padilla, "Perfect metamaterial absorber," *Phys. Rev. Lett.*, vol. 100, no. 20, May 2008, Art. no. 207402, doi: 10.1103/physrevlett.100.207402.

[3] P. Jain, K. Prakash, N. Sardana, S. Kumar, N. Gupta, and A. K. Singh, "Design of an ultra-thin hepta-band metamaterial absorber for sensing applications," *Opt. Quantum Electron.*, vol. 54, no. 9, p. 569, Sep. 2022, doi: 10.1007/s11082-022-03917-z.

[4] C. Du, D. Zhou, H.-H. Guo, Y.-Q. Pang, H.-Y. Shi, W.-F. Liu, C. Singh, S. Trukhanov, A. Trukhanov, and Z. Xu, "Active control scattering manipulation for realization of switchable EIT-like response metamaterial," *Opt. Commun.*, vol. 483, Mar. 2021, Art. no. 126664, doi: 10.1016/j.optcom.2020.126664.

[5] G. P. E. Persis, J. J. Paul, T. B. Mary, and R. C. Joy, "A compact tilted split ring multiband metamaterial absorber for energy harvesting applications," *Mater. Today, Proc.*, vol. 56, pp. 368–372, Jan. 2022, doi: 10.1016/j.matpr.2022.01.206.

[6] P. Jain, H. Chhabra, U. Chauhan, K. Prakash, A. Gupta, M. S. Soliman, M. S. Islam, and M. T. Islam, "Machine learning assisted hepta band THz metamaterial absorber for biomedical applications," *Sci. Rep.*, vol. 13, no. 1, p. 1792, Jan. 2023, doi: 10.1038/s41598-023-29024-x.

[7] A. Hoque, M. T. Islam, A. Almutairi, T. Alam, M. J. Singh, and N. Amin, "A polarization independent quasi-TEM metamaterial absorber for X and Ku band sensing applications," *Sensors*, vol. 18, no. 12, p. 4209, Nov. 2018, doi: 10.3390/s18124209.

[8] M. T. Islam, M. Cho, M. Samsuzzaman, and S. Kibria, "Compact antenna for small satellite applications," *IEEE Antennas Propag. Mag.*, vol. 57, no. 2, pp. 30–36, Apr. 2015, doi: 10.1109/map.2015.2420471.

[9] Y. Zhang, J. Lv, L. Que, G. Mi, Y. Zhou, and Y. Jiang, "A visible-infrared double band photodetector absorber," *Results Phys.*, vol. 18, Sep. 2020, Art. no. 103283, doi: 10.1016/j.rinp.2020.103283.

[10] A. Rahman, M. T. Islam, M. J. Singh, S. Kibria, and M. Akhtaruzzaman, "Electromagnetic performances analysis of an ultra-wideband and flexible material antenna in microwave breast imaging: To implement a wearable medical bra," *Sci. Rep.*, vol. 6, no. 1, p. 38906, Dec. 2016, doi: 10.1038/srep38906.

[11] Z. Gao, Q. Fan, X. Tian, C. Xu, Z. Meng, S. Huang, T. Xiao, and C. Tian, "An optically transparent broadband metamaterial absorber for radar-infrared bi-stealth," *Opt. Mater.*, vol. 112, Feb. 2021, Art. no. 110793, doi: 10.1016/j.optmat.2020.110793.

[12] N. Engheta, "Thin absorbing screens using metamaterial surfaces," in *Proc. IEEE Antennas Propag. Soc. Int. Symp.*, vol. 2, Jun. 2002, pp. 392–395, doi: 10.1109/aps.2002.1016106.

[13] P. Jain, K. Prakash, G. M. Khanal, N. Sardana, S. Kumar, N. Gupta, and A. K. Singh, "Quad-band polarization sensitive terahertz metamaterial absorber using gemini-shaped structure," *Results Opt.*, vol. 8, Aug. 2022, Art. no. 100254, doi: 10.1016/j.rio.2022.100254.

[14] P. Jain, A. K. Singh, J. K. Pandey, S. Bansal, N. Sardana, S. Kumar, N. Gupta, and A. K. Singh, "An ultrathin compact polarization-sensitive triple-band microwave metamaterial absorber," *J. Electron. Mater.*, vol. 50, no. 3, pp. 1506–1513, Mar. 2021, doi: 10.1007/s11664-020-08680-z.

[15] N. Misran, S. H. Yusop, M. T. Islam, and M. Y. Ismail, "Analysis of parameterization substrate thickness and permittivity for concentric split ring square reflectarray element," *Jurnal Kejuruteraan, J. Eng.*, vol. 23, pp. 11–16, Nov. 2012.

[16] D. Singh and V. M. Srivastava, "Dual resonance shorted stub circular rings metamaterial absorber," *AEU Int. J. Electron. Commun.*, vol. 83, pp. 58–66, Jan. 2018, doi: 10.1016/j.aeue.2017.08.034.

[17] C. M. Tran, H. Van Pham, H. T. Nguyen, T. T. Nguyen, L. D. Vu, and T. H. Do, "Creating multiband and broadband metamaterial absorber by multiporous square layer structure," *Plasmonics*, vol. 14, no. 6, pp. 1587–1592, Dec. 2019, doi: 10.1007/s11468-019-00953-6.

[18] Y. J. Kim, J. M. Kim, Y. J. Yoo, P. Van Tuong, H. Zheng, J. Y. Rhee, and Y. Lee, "Dual-absorption metamaterial controlled by electromagnetic polarization," *J. Opt. Soc. Amer. B, Opt. Phys.*, vol. 31, no. 11, p. 2744, 2014, doi: 10.1364/josab.31.002744.

[19] P. Jain, A. K. Singh, J. K. Pandey, S. Garg, S. Bansal, M. Agarwal, S. Kumar, N. Sardana, N. Gupta, and A. K. Singh, "Ultra-thin metamaterial perfect absorbers for single-/dual-/multi-band microwave applications," *IET Microw., Antennas Propag.*, vol. 14, no. 5, pp. 390–396, Apr. 2020, doi: 10.1049/iet-map.2019.0623.

[20] Y. Cheng, Y. Nie, and R. Gong, "A polarization-insensitive and omni-directional broadband terahertz metamaterial absorber based on coplanar multi-squares films," *Opt. Laser Technol.*, vol. 48, pp. 415–421, Jun. 2013, doi: 10.1016/j.optlastec.2012.11.016.

[21] K. P. Kaur, T. Upadhyaya, M. Palandoken, and C. Gocen, "Ultrathin dual-layer triple-band flexible microwave metamaterial absorber for energy harvesting applications," *Int. J. RF Microw. Comput.-Aided Eng.*, vol. 29, no. 1, Jan. 2019, Art. no. e21646, doi: 10.1002/mmce.21646.

[22] C. Tong, J. Liu, and Q. H. Liu, "Mixed finite element numerical mode matching method for designing infrared broadband polarization-independent metamaterial absorbers," *Opt. Exp.*, vol. 30, no. 25, p. 45031, 2022, doi: 10.1364/oe.472491.

[23] A. Reineix and B. Jecko, "Analysis of microstrip patch antennas using finite difference time domain method," *IEEE Trans. Antennas Propag.*, vol. 37, no. 11, pp. 1361–1369, Nov. 1989, doi: 10.1109/8.43555.

[24] H. M. El Misilmani, T. Naous, and S. K. Al Khatib, "A review on the design and optimization of antennas using machine learning algorithms and techniques," *Int. J. RF Microw. Comput.-Aided Eng.*, vol. 30, no. 10, Oct. 2020, Art. no. e22356, doi: 10.1002/mmce.22356.

[25] M. A. Bessa, P. Glowacki, and M. Houlder, "Bayesian machine learning in metamaterial design: Fragile becomes supercompressible," *Adv. Mater.*, vol. 31, no. 48, Nov. 2019, Art. no. 1904845, doi: 10.1002/adma.201904845.

[26] V. L. Deringer, M. A. Caro, and G. Csányi, "Machine learning interatomic potentials as emerging tools for materials science," *Adv. Mater.*, vol. 31, no. 46, Nov. 2019, Art. no. 1902765, doi: 10.1002/adma.201902765.

[27] S. K. Patel, J. Surve, V. Katkar, J. Parmar, F. A. Al-Zahrani, K. Ahmed, and F. M. Bui, "Encoding and tuning of THz metasurface-based refractive index sensor with behavior prediction using XGBoost regressor," *IEEE Access*, vol. 10, pp. 24797–24814, 2022, doi: 10.1109/ACCESS.2022.3154386.

[28] S. K. Patel, J. Parmar, V. Katkar, F. A. Al-Zahrani, and K. Ahmed, "Ultra-broadband and polarization-insensitive metasurface absorber with behavior prediction using machine learning," *Alexandria Eng. J.*, vol. 61, no. 12, pp. 10379–10393, Dec. 2022, doi: 10.1016/j.aej.2022.03.080.

[29] S. R. Thummaluru, N. Mishra, and R. K. Chaudhary, "Design and analysis of an ultrathin triple-band polarization independent metamaterial absorber," *AEU Int. J. Electron. Commun.*, vol. 82, pp. 508–515, Dec. 2017, doi: 10.1016/j.aeue.2017.10.024.

[30] G. Deng, T. Xia, J. Yang, and Z. Yin, "Triple-band polarisation-independent metamaterial absorber at mm wave frequency band," *IET Microw., Antennas Propag.*, vol. 12, no. 7, pp. 1120–1125, Jun. 2018, doi: 10.1049/iet-map.2017.0126.

[31] K. P. Kaur and T. Upadhyaya, "Wide-angle and polarisation-independent tri-band dual-layer microwave metamaterial absorber," *IET Microw., Antennas Propag.*, vol. 12, no. 8, pp. 1428–1434, Jul. 2018, doi: 10.1049/iet-map.2017.0990.

[32] F. S. Jafari, M. Naderi, A. Hatami, and F. B. Zarrabi, "Microwave Jerusalem cross absorber by metamaterial split ring resonator load to obtain polarization independence with triple band application," *AEU Int. J. Electron. Commun.*, vol. 101, pp. 138–144, Mar. 2019, doi: 10.1016/j.aeue.2019.02.002.

[33] K. Kumari, N. Mishra, and R. K. Chaudhary, "An ultra-thin compact polarization insensitive dual band absorber based on metamaterial for X-band applications," *Microw. Opt. Technol. Lett.*, vol. 59, no. 10, pp. 2664–2669, Oct. 2017, doi: 10.1002/mop.30797.

[34] A. D. Gordon, L. Breiman, J. H. Friedman, R. A. Olshen, and C. J. Stone, "Classification and regression trees," *Biometrics*, vol. 40, no. 3, p. 874, Sep. 1984, doi: 10.2307/2530946.

[35] Y. An, X. Wang, Z. Qu, T. Liao, and Z. Nan, "Fiber Bragg grating temperature calibration based on BP neural network," *Optik*, vol. 172, pp. 753–759, Nov. 2018, doi: 10.1016/j.ijleo.2018.07.064.

[36] T. Cover and P. Hart, "Nearest neighbor pattern classification," *IEEE Trans. Inf. Theory*, vol. IT-13, no. 1, pp. 21–27, Jan. 1967, doi: 10.1109/TIT.1967.1053964.

[37] G. Biau, "Analysis of a random forests model," *J. Mach. Learn. Res.*, vol. 13, pp. 1063–1095, Apr. 2012.

[38] S. Adusumilli, D. Bhatt, H. Wang, V. Devabhaktuni, and P. Bhattacharya, "A novel hybrid approach utilizing principal component regression and random forest regression to bridge the period of GPS outages," *Neurocomputing*, vol. 166, pp. 185–192, Oct. 2015, doi: 10.1016/j.neucom.2015.03.080.

[39] P. Jain, H. Chhabra, U. Chauhan, D. K. Singh, T. M. K. Anwer, S. H. Ahammad, M. A. Hossain, and A. N. Z. Rashed, "Multiband metamaterial absorber with absorption prediction by assisted machine learning," *Mater. Chem. Phys.*, vol. 307, Oct. 2023, Art. no. 128180, doi: 10.1016/j.matchemphys.2023.128180.

[40] A. Criminisi, "Decision forests: A unified framework for classification, regression, density estimation, manifold learning and semi-supervised learning," *Found. Trends Comput. Graph. Vis.*, vol. 7, nos. 2–3, pp. 81–227, 2011, doi: 10.1561/0600000035.
[41] A. Kadiyala and A. Kumar, "Applications of Python to evaluate the performance of bagging methods," *Environ. Prog. Sustain. Energy*, vol. 37, no. 5, pp. 1555–1559, Sep. 2018, doi: 10.1002/ep.13018.
[42] A. Shehadeh, O. Alshboul, R. E. Al Mamlook, and O. Hamedat, "Machine learning models for predicting the residual value of heavy construction equipment: An evaluation of modified decision tree, LightGBM, and XGBoost regression," *Autom. Construct.*, vol. 129, Sep. 2021, Art. no. 103827, doi: 10.1016/j.autcon.2021.103827.
[43] J. T. Hancock and T. M. Khoshgoftaar, "CatBoost for big data: An interdisciplinary review," *J. Big Data*, vol. 7, no. 1, p. 94, Dec. 2020, doi: 10.1186/s40537-020-00369-8.
[44] C. Persson, P. Bacher, T. Shiga, and H. Madsen, "Multi-site solar power forecasting using gradient boosted regression trees," *Sol. Energy*, vol. 150, pp. 423–436, Jul. 2017, doi: 10.1016/j.solener.2017.04.066.
[45] X. Li, W. Li, and Y. Xu, "Human age prediction based on DNA methylation using a gradient boosting regressor," *Genes*, vol. 9, no. 9, p. 424, Aug. 2018, doi: 10.3390/genes9090424.

PRINCE JAIN received the Doctor of Philosophy (Ph.D.) degree from the Punjab Engineering College (Deemed to be University), Chandigarh, India, through the Visvesvaraya Ph.D. Scheme Fellowship. He is currently an Assistant Professor with the Mechatronics Engineering Department, Parul Institute of Technology, Parul University, Vadodara, India. He is the author or coauthor of about 16 research journal articles, 20 conference papers, and a few book chapters on various topics related to antennas, machine learning, and metamaterials. He has contributed as a Peer Reviewer for prestigious publishers, including IEEE, Elsevier, IOPscience, Wiley, PIER, Emerald, and PLOS. His research interests include machine learning, artificial intelligence, optimization techniques, metamaterial absorbers/antennas at RF, THz, and visible frequencies, material science, nanotechnology, and biomedical signal processing. He is serving as an Academic Editor for *Journal of Electrical and Computer Engineering* (Hindawi) and *PLOS One*. He is also serving as a Topical Advisory Panel Member for *Micromachines* and *Materials* (MDPI).

HIMANSHU CHHABRA received the B.Tech. degree in electronics and communication engineering, the M.Tech. degree in control and instrumentation engineering, and the Ph.D. degree in instrumentation and control engineering, in 2012, 2014, and 2021, respectively. He is currently an Assistant Professor with the Mechatronics Engineering Department, Parul University, Vadodara, India. He has authored or coauthored various scientific articles in the field of robotics, biomedical signal processing, metamaterial absorber, and MPPT design for solar PV. His research interests include control system design, machine learning, artificial intelligence, and optimization techniques.

URVASHI CHAUHAN received the B.Tech. degree in electronics and instrumentation engineering from UPTU Lucknow, in 2011, and the M.Tech. and Ph.D. degrees in instrumentation and control engineering from the Netaji Subhas Institute of Technology, University of Delhi, in 2015 and 2022, respectively. She is currently an Associate Professor with the Electronics and Communication Engineering Department, Faculty of Engineering and Technology, Parul University, Vadodara. She has authored or coauthored various scientific articles in the field of renewable energy sources. Her research interests include renewable energy sources, solar energy, and non-linear control and optimization techniques.

KRISHNA PRAKASH received the B.Tech. degree in electronics and communication engineering from Punjab Technical University, Punjab, India, the M.Tech. degree in nanoscience and technology from Guru Gobind Singh Indraprastha University, New Delhi, India, and the Ph.D. degree from SRM University, Andhra Pradesh, India. He was awarded the Visvesvaraya Ph.D. Scheme Fellowship to carry out his Ph.D. work in nano-electronics with the Punjab Engineering College (Deemed to be University), Chandigarh, India. He is currently a Professor with the ECE Department, NRI Institute of Technology, Agiripalli, Krishna, Andhra Pradesh, India. From his research activities and various collaborative works, he has been able to publish 14 international journals, seven conference papers, and one book chapter. His research interests include material synthesis, and device simulation, such as solar cells, ballistic rectifiers, thermoelectric rectifiers, and nano-electronics devices by using simulation software Silvaco TCAD and SCAPs-1D, as well as its fabrication.

PIYUSH SAMANT received the Ph.D. degree in biomedical imaging from the Thapar Institute of Engineering and Technology, Patiala, India, in 2020. He has vast experience in medical image analysis and artificial intelligence. He is currently a Data Scientist with Mirxes Laboratories Pvt. Ltd., Singapore. In the past, he served in various positions in the teaching and research industry. His major research interests include cancer diagnosis, biomedical imaging, retinal and diabetes diagnosis, medical device development, machine learning, and deep learning. He is also the Director General of the International Forum for Educators & Researchers (IFER), London. He is the Editor-in-Chief LLP under Beyond-Leer Imprint at Kohli Media.

DHIRAJ KUMAR SINGH received the Ph.D. degree in satellite image and signal processing (electronics and communication engineering) from the Punjab Engineering College (Deemed to be University), Chandigarh, India, in 2020, sponsored by the Defense Research and Development Organization (DRDO), Chandigarh, and the Ph.D. degree from the Indian Institute of Technology (IIT) Bombay, in 2023. He was a Scientist. Since 2012, he has had more than ten years of experience in teaching, and research and development. He is currently an Assistant Professor with the Kalpana Chawla Centre for Research in Space Science and Technology, Chandigarh University, which was inaugurated by the Defence Minister Shri. Rajnath Singh, in January 2022, which is said to be an essential step toward strengthening the country's space and geospatial sector. He has contributed to many projects sponsored by DRDO and the Department of Science and Technology, India. He is the author and a reviewer of many peer-reviewed book chapters and journal articles. His research interests include satellite sensor calibration, CubeSat designing, remote sensing and GIS, and digital image and signal processing.

MOHAMED S. SOLIMAN (Senior Member, IEEE) received the Ph.D. degree in communications engineering from the Graduate School of Engineering, Osaka University, Japan. He was granted many research projects from the Deanship of Scientific Researches, Taif University, Saudi Arabia. He has been recognized as a Distinguished Researcher (one of the hundred most active researchers) by the Deanship of Scientific Research, Taif University, in 2023. He was rewarded the Distinguished Researchers Supporting Project and the Scientific Publication Reward for 2023 from the Deanship of Scientific Research, Taif University. He is an Associate Professor with the Department of Electrical Engineering, College of Engineering, Taif University. He is the author or coauthor of more than 140 papers indexed in Scopus and WOS databases and five book chapters. His research interests include wireless communications, phased and timed array signal processing, UWB antennas, MIMO antennas, dielectric resonant antennas, optimization techniques in antenna design, antenna measurement techniques, metamaterial structures, biosensors, RF energy harvesting systems, and numerical methods in electromagnetics. He is a Senior Member of the IEEE-MTT/AP Society. He serves as a TPC member for many international conferences. He serves as a Reviewer for many scientific journals, such as PIER journals—PhotonIcs and Electromagnetics Research Symposium, *International Journal of RF and Microwave Computer-Aided Engineering* (Wiley Hindawi Partnership), and *Wireless Personal Communications* (Springer).

MOHAMMAD TARIQUL ISLAM (Senior Member, IEEE) is currently a Professor with the Department of Electrical, Electronic and Systems Engineering, Universiti Kebangsaan Malaysia (UKM), and a Visiting Professor with the Kyushu Institute of Technology, Japan. He has supervised about 50 Ph.D. theses and 30 M.Sc. theses, and has mentored more than ten postdoctoral and visiting scholars. He has developed the Antenna Measurement Laboratory which includes antenna design and measurement facility till 40 GHz. He is the author or coauthor of about 600 research journal articles, nearly 250 conference papers, and a few book chapters on various topics related to antennas, metamaterials, and microwave imaging with 25 inventory patents filed. Thus far, his publications have been cited 14,000 times and his H-index is 53 (Source: Scopus). His Google Scholar citation is 22500 and his H-index is 62. His research interests include communication antenna design, metamaterial, satellite antennas, and microwave imaging. He has been serving as an Executive Committee Member for the IEEE AP/MTT/EMC Malaysia Chapter, from 2019 to 2020. He is a fellow of IET, U.K., and a Senior Member of IEICE, Japan. He was a recipient of more than 40 research grants from the Malaysian Ministry of Science, Technology and Innovation, the Ministry of Education, the UKM Research Grant, and international research grants from Japan, Saudi Arabia, and Kuwait. He received several International Gold Medal Awards, the Best Invention in Telecommunication Award for his research and innovation, and the Best Researcher Award from UKM. He was a recipient of the 2018, 2019, and 2020 IEEE AP/MTT/EMC Malaysia Chapter, Excellent Award. He also won the Best Innovation Award and the Best Researcher Award by UKM, in different years. He was a recipient of the Publication Award from the Malaysian Space Agency, for several years. He was an Associate Editor of *Electronics Letters* (IET). He also serves as the Guest Editor for *Sensors* and *Nanomaterials* and an Associate Editor for IEEE Access. He has been serving as a Chartered Professional Engineer (C.Eng.).